Jurnal Teknologi

Full Paper

MATHEMATICAL MODEL FOR CHIP GEOMETRY CALCULATION IN FIVE-AXIS MILLING

Hendriko*

Mechatronic Department, Politeknik Caltex Riau

Article history
Received
27 April 2015
Received in revised form
15 June 2015
Accepted
25 November 2015

*Corresponding author
hendriko@pcr.ac.id

Abstract

This paper presents the method to calculate the geometries of instantaneous chip in five-axis milling. The inclination angle changes in between two consecutive CC-points were taken into account in the calculation. In the first stage, the engagement angle, the axial depth of cut and cut width were determined through the mapping technique. The engagement point of the Work piece Coordinate System (WCS) was mapped to a Tool Coordinate System (TCS). In the second stage, the engagement angle and depth of cut, which were defined in the first stage were then used as a primary input to obtain the cut thickness and cut width. Two simulation tests have been presented to verify the ability of the proposed model to predict the cut geometry. The first tests revealed that the inclination angle makes the size of the cut thickness and cut width fluctuate. The cut width increased when the tool inclination angle increased. For the cut thickness, its magnitude was influenced by two effects, the orientation effect and the tooth path effect. The final result was a compromise between these two effects. In the second simulation test, the proposed model was successfully implemented to support the feedrate scheduling method.

Keywords: Inclination angle, cutting force, five axis milling, chip geometry

1.0 INTRODUCTION

Contrary to the advancement in machine tool technology and milling tool development, machining parameters such as feedrate, cutting speed, width of cut, are selected conventionally to avoid the risk of damaging workpiece, cutting tool and even the machine tool during the machining process. There is an increasing demand for virtual machining application that are capable in predicting the performance measures such as cutting forces, surface quality, tool deflection and power demands. Virtual machining has two main parts, geometric modeling and process modeling. The process modeling needs precise information about the chip geometry from the geometric modeling to predict the cutting forces. Information on the instantaneous cutting forces can be used to increase the machining efficiency by maximized amount of material at every instant of the cutting process, thus reducing the overall cutting time. From the literature [1-11], it can be seen that research works for Cutter Worpiece Engagement (CWE) extraction can be classified into three main methods, solid modeler based approach, polyhedral based method and vector based method. There is always a tradeoff between the complexity of computation and accuracy in this approach.

Some studies in Solid model based CWE extraction for supporting process modeling have been presented by [1-3]. Another method that is widely used in geometric modeling is vector based model [4-8]. The model represents the workpiece as a set of position and direction vectors. Another alternative for modeling CWE that is starting to receive more attention are Polyhedral Models. Several researches [9-11] on polyhedral based CWE extraction method for supporting the process modeling have been reported.

This paper presents a method to generate the instantaneous CWE during 5-axis milling. Development of CWE in 5-axis milling becomes more complicated due to the two additional rotation tool motions. In this research, the methodology as developed by Aras and

Hoi [13] for obtaining CWE in 3-axis milling is applied for 5-axis milling. Then, the model developed by Gani et al. [14] was used to define the instantaneous chip geometry. And the tool orientation (inclination angle) change in between two consecutive CC point is taken into account.

2.0 MATHEMATICAL MODEL OF CHIP GEOMETRY

In this section, mathematical equations to define the geometry of the chips were derived. Figure 1a [12] shows an illustration of the cutting tool movement and material removed. For conventional milling, the tool is set without the inclination angle (a=0), and hence the shape of cutting tool remains a circle. This condition produces a square shape of chip geometry as depicted in Figure 1b. However, when a constant inclination angle (a) is introduced to the cutting tool, the shape of the cutting tool is not a circle anymore. It becomes an ellipse with a minor axis is equal to R, and a major axis is equal to R/cosa, as shown in Figure 1c. The shape of the cross cutting is not a square anymore, but has now become a trapezium. Another condition shown in Figure 4d, when the tool orientation continuously changes, the shape of cutting tool is also changed gradually. The major axis becomes R/cosal, where al is an instantaneous inclination angle.

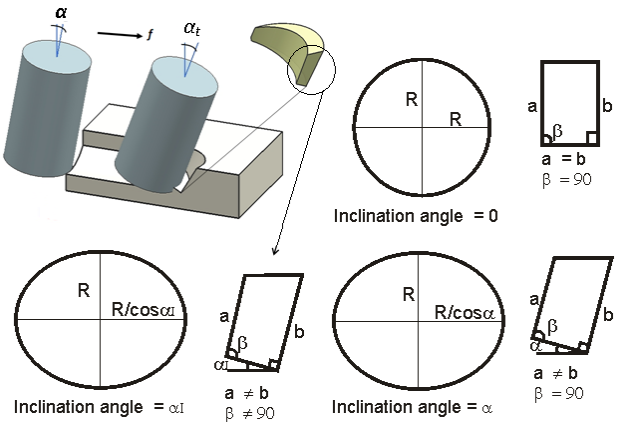

Figure 1 Cutting tool and cross cut of chip shape. a) 3D model of cutting tool and chip; b, c, d) top view of actual cutting tool shape and front view of instantaneous cross cut of chip shape at various inclination angles [12]

The equations of the ellipse can be expressed as shown in Eq.(1) and can be rearranged as shown in Eq.(2),

$$\frac{X^2}{R^2/\cos^2 a} + \frac{Y^2}{R^2} = 1 \qquad 1$$

$$\cos^2 a . X^2 + Y^2 = R^2 \qquad 2$$

When applying inclination angle, the depth of cut varies with the value of the tool motion angle. The depth of cut, formed the ellipse shape as the shape of the bottom side of the cutting tool. Two possible conditions may occur, first, when the cutting edge is located at the point when the engagement angle is equal to zero, which will occur if the depth of cut is greater than or equal to *R.sina.sinφ* as shown in Figure 2a. Otherwise, the engagement starts from a certain value of tool motion angle as depicted in Figure 2b.

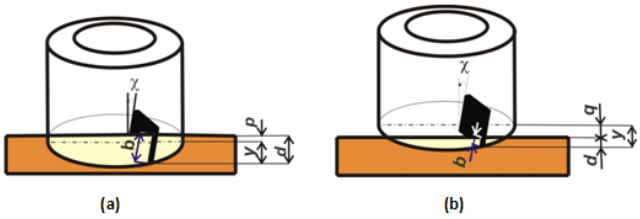

Figure 2 Side view of chip formation, a) when d ≥ R.sina.sinφ, b) when d < R.sina.sinφ

The engagement angle and depth of cut which have been determined in the previous section is then used as the primary input to obtain the instantaneous size of cut thickness, depth of cut, and also cut width. Determination of chip geometry for continuous tool orientation change is not as simple as when milling with a constant tool orientation.

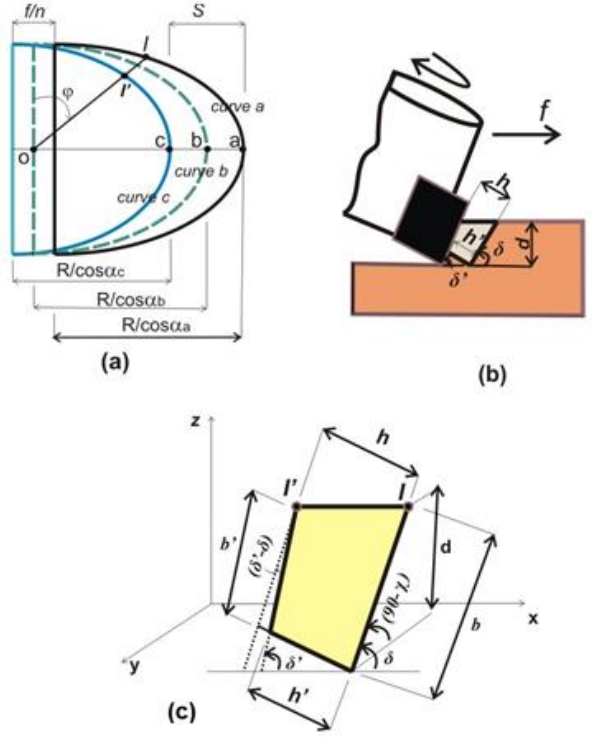

Figure 3 a) top view and, b) front view of cut formation, c) geometry of instantaneous chip

The general view of the cut geometry when machining using insert tool edge is depicted in Figure 3. In this case, the CWE start at the engagement angle is equal to zero. When a point in the cutting tool engage with the workpiece, it will follow the path as shown in Figure 3a. The shape of the path is influenced by several

variables: the actual shape of the cutting tool as expressed in Eq.(1) and Eq.(2), feed rate (f), number of teeth (n), and feed motion angle or engagement angle (φ). In the milling process, the chip geometry can be calculated by determining the tool motion path. According to Kumanchik and Schmitz [13] the chip thickness in milling is defined as the distance between the current tooth's path and the previous tooth's path along the line segment connecting the tool center to the current tooth's cutting edge. However, this definition was only applicable for machining with perpendicular tool orientation. Otherwise, the orientation angle should be taken into consideration as another factor that influences the size of cut thickness. It can be seen in Figure 3b that the tool orientation makes the cut thickness thinner than the distance of the two consecutive tooth paths.

Due to the continuously change of the inclination angle, it makes the major axis length of curve 'a' is different with the major axis length of curve 'c'. Increasing inclination angle will longer the major axis of the curve. To calculate the distance between these two curves, the dummy curve (curve 'b'), which represents the average motion of both curves, was created and put in between them. Its major axis was computed using the average inclination angle of curve 'a' and the average inclination angle of curve 'c'. Below are the equations of the instantaneous inclination angle curves.

$$\alpha_{a(\varphi)} = \alpha_p + (\varphi - \varphi_I)\Delta\alpha \quad (3)$$

$$\alpha_{c(\varphi)} = \alpha_a - \left(\frac{360}{n}\right)\Delta\alpha \quad (4)$$

$$\alpha_{b(\varphi)} = (\alpha_a + \alpha_c)/2 \quad (5)$$

where the inclination change rate (Δα) in every degree of tool rotation was obtained as follow,

$$\Delta\alpha = \frac{\left((\mu_n - \mu_{n+1}) + (\alpha_n - \alpha_{n+1})\right).f}{360.L} \quad (6)$$

The equation of the dummy ellipse was obtained using Eq. (2) with the X shifted to S/2,

$$\cos^2\alpha_{b(\varphi)}.\left(X - \frac{S}{2}\right)^2 + Y^2 = R^2 \quad (7)$$

where *S* is the distance between major axis of curve 'a' (at point a) and major axis of curve 'c' (at point 'c'), and it is calculated using the equation as follow,

$$S = \frac{f}{n} + \frac{R}{\cos\alpha_{a(\varphi)}} - \frac{R}{\cos\alpha_{c(\varphi)}} \quad (8)$$

For an ellipse, $Y = X\,cot\,\varphi$. It was substituted into Eq.(9) and then it yielded to,

$$\cos^2\alpha_{b(\varphi)}.\left(X - \frac{S}{2}\right)^2 + (X.\cot\varphi)^2 = R^2 \quad (9)$$

$$(\cos^2\alpha_b + \cot^2\varphi)X^2 - (S.\cos^2\alpha_b)X + \left(\frac{S}{2}\right)^2 - R^2 = 0 \quad (10)$$

Thus, the instantaneous distance between points *I* to *I'* in X abscissa, as shown in Figure 3, was determined using the second order of quadric Eq.(10), and it was derived as follow,

$$\Delta X_{(\varphi)} = \frac{S.\cos^2\alpha_{b(\varphi)}}{\left(\cos^2\alpha_{b(\varphi)} + \cot^2\varphi\right)} \quad (11)$$

$$\Delta X_{(\varphi)} = \left(\frac{f}{n} + \frac{R}{\cos\alpha_{a(\varphi)}} - \frac{R}{\cos\alpha_{c(\varphi)}}\right)\left(\frac{\cos^2\alpha_{b(\varphi)}\sin^2\varphi}{\cos^2\alpha_{b(\varphi)}\sin^2\varphi + \cos^2\varphi}\right) \quad (12)$$

Now, the distance of I' to I was calculated as follow,

$$I'I_{(\varphi)} = \frac{\Delta X_{(\varphi)}}{\sin\varphi} \quad (13)$$

Then cut thickness at the top side was determined as follow,

$$h_{(\varphi)} = I'I\sin\delta = I'I\sin(\lambda - \alpha_{(\varphi)}) \quad (14)$$

$$h_{(\varphi)} = I'I\sin(\lambda - \alpha_p - (\varphi - \varphi_I)\Delta\alpha) \quad (15)$$

The depth of cut obtained in the previous section (Eq. 14) is only valid for φ_I. To know the whole geometry of chip, it need to define the depth of cut as a function of tool motion. The magnitude of the instantaneous depth of cut is influenced by two factors: the initial depth of cut at entry point (p) and y value of the ellipse at the bottom of the tool as shown in Figure 5a.

$$d_I = p + y_I = p + R\sin\alpha_p\sin\varphi_I \quad (16)$$

$$p = d_I - R\sin\alpha_p\sin\varphi_I \quad (17)$$

And then the depth of cut as a function of engagement angle can be determined as follow,

$$d_{(\varphi)} = p + y_{(\varphi)} = p + R\sin\alpha_{a(\varphi)}\sin\varphi \quad (18)$$

$$d_{(\varphi)} = d_I - R(\sin\alpha_p\sin\varphi_I - \sin(\alpha_p + (\varphi - \varphi_I)\Delta\alpha)\sin\varphi) \quad (19)$$

Another parameter that need to be defined is the cut width. Since the cutting tool used helical angle (χ), the cut width become larger. Therefore, the front side of cut width at point I is given by,

$$b_{(\varphi)} = \frac{d_{(\varphi)}}{(\sin\delta_{(\varphi)}.\cos\chi)} \quad (20)$$

$$b_{(\varphi)} = \frac{d_I - R(\sin\alpha_p\sin\varphi_I - \sin(\alpha_p - (\varphi_I - \varphi)\Delta\alpha)\sin\varphi)}{(\sin(\lambda - \alpha_p + (\varphi - \varphi_I)\Delta\alpha).\cos\chi)} \quad (21)$$

Because the tool orientation change continuously, it cause the cut width at point I' is different than that at point I. The cut width at the back side is given as follow

$$b'_{(\varphi)} = \frac{\left(b_{(\varphi)} - h_{(\varphi)}\tan\alpha_{a(\varphi)}\right)}{\cos(\delta - \delta')} \quad (22)$$

$$b'_{(\varphi)} = \frac{\left(b_{(\varphi)} - h_{(\varphi)}\tan\alpha_{a(\varphi)}\right)}{\cos\left(\left(\lambda - (\alpha_{a(\varphi)} - \left(\frac{360}{n}\right)\Delta\alpha)\right) - (\lambda - \alpha_{a(\varphi)})\right)} \quad (23)$$

$$b'_{(\varphi)} = \frac{\left(b_{(\varphi)} - h_{(\varphi)}\tan\alpha_{a(\varphi)}\right)}{\cos\left(\left(\frac{360}{n}\right)\Delta\alpha\right)} \quad (24)$$

Again, due to the tool orientation change, the cut thickness at the bottom side is different than that at the top side. It is defined as follow,

$$h'_{(\varphi)} = h_{(\varphi)} - b'_{(\varphi)} \sin(\delta - \delta') = \quad (25)$$

$$h_{(\varphi)} - b'_{(\varphi)} \sin\left(\left(\frac{360}{n}\right)\Delta\alpha\right) \quad (26)$$

For practical purposes, it is simpler to use the average cut width and the average cut thickness, and the equations change to become as follow,

$$b_{av(\varphi)} = \frac{1}{2}\left(b_{(\varphi)} + b'_{(\varphi)}\right) \quad (27)$$

$$b_{av(\varphi)} = \frac{1}{2}\left(b_{(\varphi)} + \frac{\left(b_{(\varphi)} - h_{(\varphi)} \tan \alpha_{a(\varphi)}\right)}{\cos\left(\left(\frac{360}{n}\right)\Delta\alpha\right)}\right) \quad (28)$$

$$h_{av(\varphi)} = \frac{1}{2}\left(h_{(\varphi)} + h'_{(\varphi)}\right) \quad (29)$$

$$h_{av(\varphi)} = h_{(\varphi)} - \frac{1}{2} b'_{(\varphi)} \sin\left(\left(\frac{360}{n}\right)\Delta\alpha\right) \quad (30)$$

Finally, the cross cut area is calculated by multiplying the average cut thickness by the average cut width.

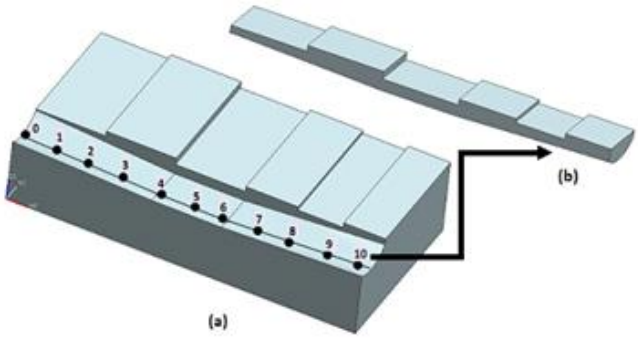

Figure 4 Part model with variation in axial depth of cut, a) the in process workpiece, b) removal material

3.0 APPLICATION AND DISCUSSION

To verify the ability of the proposed model to predict the chip geometry, the formulae derived in the previous section were examined. Two types of part model with variation of axial depth of cut were machined. In this simulation, the machining was performed using two teeth flat-end cutter with radius (R) 6.25 mm, feed rate (f) 0.2 mm/rev. and cutting speed 1000 rpm.

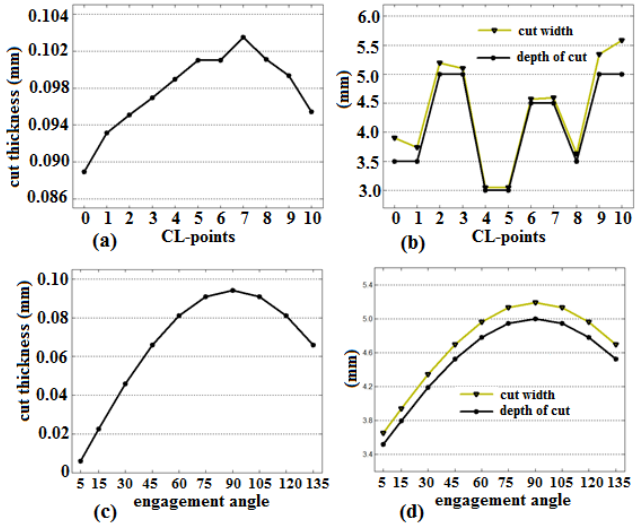

Figure 5 Simulation data for the first model, a) cut thickness at every CL points with φ = 90; b) cut width and depth of cut at every CC points with φ = 90; c) cut thickness at CL-2 with 5 ≤ φ ≤ 135; d) cut width and depth of cut at CL-2 with 5 ≤ φ ≤ 135

For the first test, there were eleven cutter location (CL) points used to check the effect of inclination angle change to the cut thickness and cut width. The distance between CL-points was set 10 mm. The inclination angle at CL-0, CL-4, CL-6, CL-10 were given 25, 0, 0, 25, respectively. The tool adjusted its orientation gradually to reach the defined inclination angle at every CL-points. Using Eq.(6), it was found that the tool reduced its inclination with the inclination change rate 0.125/rev when the tool movee from CL-0 ($\alpha_0 = 25$) to CL-4 ($\alpha_4 = 0$). Thereafter, the tool maintain its orientation when moving from CL-4 ($\alpha_4 = 0$) to CL-6 ($\alpha_6 = 0$). Finally, It increased its inclination angle with the same inclination change rate when the tool moved from CL-6 ($\alpha_6 = 0$) to CL-10 ($\alpha_{10} = 25$). Due to the tool orientation dynamically change, it produced irregular profile at the machined surface and the bottom face of material removed as shown in Figure 4.

Graph of the cut thickness (h_{av}) as a function of CL-points is presented in Figure 5a. Cut thickness increased as well as the inclination angle decreased. Then, it maintained its size when the inclination angle was fixed (from point 5 to point 6). However, when the tool was located at point 7, the cut thickness still increased even though the inclination increased. It started to decrease when the cutting tool moved from point 8 to point 10. The existence of inclination angle made the cut thickness smaller. It is called the orientation effect. However, increasing the inclination angle also increased the distance between two consecutive tooth path (distance I to I') and made the cut thickness larger. This condition is called the toot path effect. The final result was a compromise between these two effects. In this test, the orientation effect gave more dominant effect than the tool path effect. So, it can be concluded that increasing the tool inclination angle tend to decrease the cut thickness.

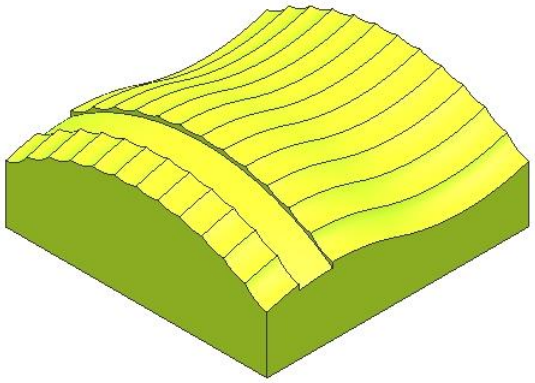

Figure 6 The second part model with free form surface

Figure 5b presented the cut width and the axial depth of cut at selected CL-points. It shows clearly that the size of cut width (b_{av}) mostly influenced by the depth of cut. However, the depth of cut was not the only factor. It can be seen at several pairs of points (CL-0/CL-1, CL-2/ CL-3, and CL-9/CL-10) which have similar the depth of cut but produced different the cut width. These variations were believed because of the inclination angle change. When the inclination angle decreased from CL-0 to CL-1 or from CL-2 to CL-3, it made $b_{av0} > b_{av1}$ or $b_{av2} > b_{av3}$. For the case when the inclination angle increased from CL-9 to CL-10, it made $b_{av9} < b_{av10}$. The cut widths at CL-4, CL-5, CL-6 maintain theirs size because the inclination angle were fixed. On the other hand, the cut width were bigger slightly as compared to the depth of cut due to the existence of helical angle.

For the next test, CL point 2 (CL-2) was selected for analyzing the effect of engagement angle or tool motion to the chip geometry. Figure 5c illustrated the cut thickness data as a function of engagement angle. Initially, the cut thickness increased gradually with the gradual increase in engagement angle until it reachedd the maximum size at engagement angle was equal to 90, Aafter that, they started become smaller. The eengagement angle gave relatively the same effect to the cut width and depth of cut. The depth of cut and cut width for this test were presented in Figure 5d. It can be observed that CWE occurred at a certain value of the depth of cut. The existence of inclination angle and helical angle made the cut width was larger than the depth of cut. It can be taken into conclusion that larger the inclination angle, the larger the cut width.

Figure 6 showed the second part model with a free-form surface. The second simulation test was performed using the same cutting condition and cutting tool. This test was aimed to obtain the optimum feedrate based on the cut area data at every CL-point. The CL-points data were generated using Siemens NX, and it gave 40 CL-points for one strip machining as shown in Figure 6. The inclination angle at every CL-point was maintained at 5. In this case, the tool continuously changed its orientation with the inclination change rate 0.111o/rev.

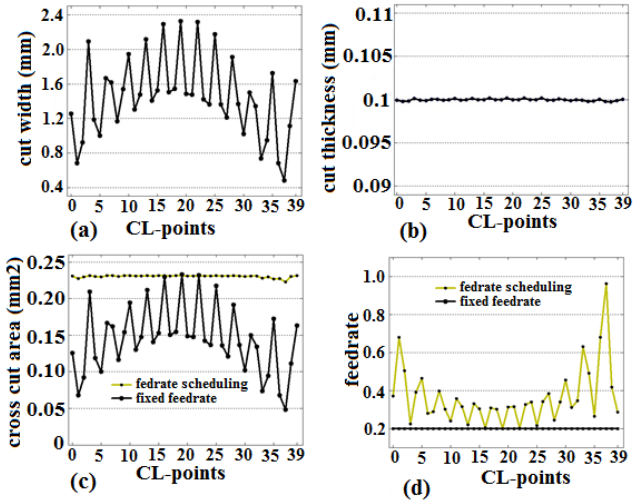

Figure 7 Simulation data for the second model; (a) cut width; (b) cut thickness; (c) cross cut area, (d) federate

Figure 7(a) presented the cut width data at every CL points, in which the cut width fluctuated while the tool moves along the inclined tool path. Figure 7(b) illustrates the cut thickness at every CL points. It can be seen that cut thickness only fluctuates slightly. This small fluctuation was due to the constant inclination angle applied at every CL-point. The small variation in the cut thickness was influenced by the variation of the cut width. When the cut width increased, the cut thickness also increased and vice versa. Figure 7c and Figure 7d showed the cut area data and feedrate at every CL-point. When the fixed feedrates were applied at all CL points, irregular shapes of cross cut area data were generated. The graph of the cut area resembled the graph of cut width. It was due to the cut thickness was relatively constant.

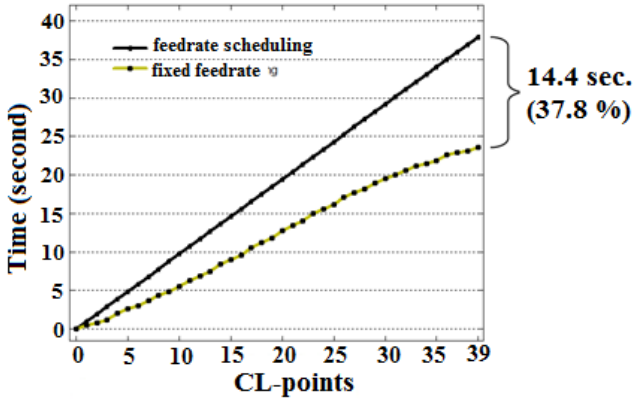

Figure 8 The machining time before and after feedrate scheduling

Since the chip geometry parameter is one of the most important parameters in the cutting force prediction, adjusting feedrate can be performed by selecting the chip geometry as reference parameter. Since there is a

linear relationship between feedrate and the cut area, then feedrate at every CL points can be adjusted to a value which gives the cross cut area near by the reference cross cut area. Based on the data shown in Figure 11(c), the scheduled feedrates at every CL points were calculated and presented in Figure 7d. The maximum cross cut area when machining using fixed feedrate was chosen as the reference cut area. In this paper, the dynamic effect of the feedrate scheduling to the machining process were not considered. This concern will be part of our future study.

The simulation machining time before and after feedrate scheduling was compared as depicted in Figure 8. It can be seen that the total machining time was successfully reduced from 37.9 second to 23.5 second, or saving until 37.8%, by feedrate scheduling.

4.0 CONCLUSION

In this study, the geometries of the cross section of instantaneous CWE in five axis milling have been defined. Chip geometry calculation of continuous tool orientation change is not as simple as milling without the inclination angle or at constant tool orientation. Two simulation tests were presented to verify the ability of the proposed model to predict the chip geometry. The first tests revealed that the inclination angle make the size of the average cut thickness and the average cut width become more dynamic. The cut width increased when the tool inclination angle increased. While the magnitude of cut thickness was influenced by the orientation effect and toot path effect. The final result was a compromise between these two effects. In the second simulation test, the proposed model was successfully implemented to support the feedrate scheduling method. It showed that the machining time become shorter.

References

[1] Imani, B. M., Sadeghi, M.H., Elbestawi, M.A. 1998. An improved process simulation system for ball-end milling of sculptured surfaces. *Int. J Mac. Tools Manuf*. 38(9): 1089-1107

[2] Yip-Hoi, D., Huang, X. 2006. Cutter/Workpiece engagement feature extraction from solid models for end milling. Journal of manufacturing science and engineering. *Transaction of the ASME*. 128 (1): 249-260

[3] Larue, A., Altintas, Y. 2004. Simulation of flak milling processes. Int. J. Machine Tools and Manuf. 45: 549-559.

[4] Choi, B.K., Jerrard, R. Sculptured surface machining. Theory and Applications. Kluwer Academic, Dordrecht

[5] Fussell, B .K., Jerard R. B., Hemmett J.G. 2001 Robust feedrate selection for 3-axis NC machining using discrete models. *ASME Journal of Manufacturing Science and Engineering*. 123: 214-224.

[6] Fussel, B.K., Ersoy, C., Jerard, R.B. 1992. Computer Generated CNC Machining Feedrates. *ASME Japan/USA Symposium on Flexible Automation*. 1: 377-384.

[7] Woon-Soo, Y., Jeong-Hoon, K., Han, L, Dong-Woo, C. 2002. Development of a virtual machining system, Part 3: Cutting process simulation in transient cuts. *Int. J. Mach. Tools. Manuf*. 42(15): 1617-1626.

[8] Jerard, R. B., Drysdale, R. L., Hauck, K. E., Schaudt, B., Magewick, J. 1989. Methods for detecting errors in numerically controlled machining of sculptured surfaces. *Computer Graphics and Applications, IEEE*. 9(1): 419-430.

[9] Yao, Z. 2005. Finding Cutter Engagement For Ball End Milling of Tesellated Free-Form Surfaces. Presented at ASME *International Design Engineering Technical Conferences*. DETC2005-84798

[10] Aras, E, Hoi, D. Y. 2008. Geometric modeling of cutter/workpiece engagements in three axis milling using polyhedral representations. *J. Manufacturing Science and Engineering*. 8(3): 031007.

[11] Yip-Hoi, D., Peng, X. 2007. R-Tree Localization for Polyhedral Model Based Cutter/Workpiece Engagements Calculations in Milling. Presented at ASME-CIE.

[12] Kiswanto, G., Hendriko, Duc, E. 2011. An approach for geometric modeling of cutter workpiece engagement in five-axis milling. *Proceeding of Quality in Research (QiR) 2011*, Bali, Indonesia.

[13] Kumanchik, L. M. Schmitz, T. L., 2007. Improved analytical chip thickness model for milling, *Precision Engineering*. 31: 317-324.